REVIEW

CO$_2$ conversion by reverse water gas shift catalysis: comparison of catalysts, mechanisms and their consequences for CO$_2$ conversion to liquid fuels

Yolanda A. Daza and John N. Kuhn*

Current society is inherently based on liquid hydrocarbon fuel economies and seems to be so for the foreseeable future. Due to the low rates (photocatalysis) and high capital investments (solar-thermo-chemical cycles) of competing technologies, reverse water gas shift (rWGS) catalysis appears as the prominent technology for converting CO$_2$ to CO, which can then be converted *via* CO hydrogenation to a liquid fuel of choice (diesel, gasoline, and alcohols). This approach has the advantage of high rates, selectivity, and technological readiness, but requires renewable hydrogen generation from direct (photocatalysis) or indirect (electricity and electrolysis) sources. The goal of this review is to examine the literature on rWGS catalyst types, catalyst mechanisms, and the implications of their use CO$_2$ conversion processes in the future.

1. Introduction

1.1 CO$_2$ availability and current utilization

Recently, the global carbon dioxide atmospheric concentration reached a threshold of 400 ppm, increasing the average world temperature prior to the industrial revolution by 1.5 °C. In 2013, 32.19 gigatonnes (Gt) of CO$_2$ was emitted into the atmosphere,[1] and the emissions are expected to increase to 45 Gt per year by 2040. Approximately 22% and 33% of the yearly anthropogenic emissions are absorbed into the oceans and plants, respectively, in the natural photosynthesis cycle, with the remaining 45% contributing to the increasing atmospheric concentrations.[2] A drawback with oceanic CO$_2$ absorption is that the gas is not absorbed evenly, but rather 40% of absorption occurs in the Southern Ocean.[3] By 2030, the acidification of this Ocean would likely have palpable consequences on its native organisms, which could potentially affect the food web of the area.[4] The rapidly increasing atmospheric CO$_2$ concentration and the threat it poses upon the environment has led to increased efforts to reduce or minimize CO$_2$ atmospheric emissions. Among the most widely used approaches is Carbon Capture and Storage (CCS), more commonly called sequestration. Even though the Global CCS Institute estimates that the "large" projects (>0.8 Mt – mega tonnes – for coal-based power plants or >0.4 Mt for other industrial facilities), under evaluation could potentially have a sequestration capacity of 81.5 Mt of CO$_2$/year;[5] the actual operational projects only reach a 28.4 Mt sequestration capacity.[6] Furthermore, current CO$_2$ utilizations for industrial processes, such as urea and salicylic acid synthesis (Fig. 1), do

not exceed 120 Mt per year.[7,8] Production of CO$_2$ is more than 150 times higher than its current use and potential sequestration capability (Table 1, current methods). Due to its large-scale, long-term planning of a combination of methods and technologies at all levels of society from industry to individual households, sequestration should be used if we are to significantly reduce CO$_2$ emissions or manufacture it into fuels and chemicals.[5,7]
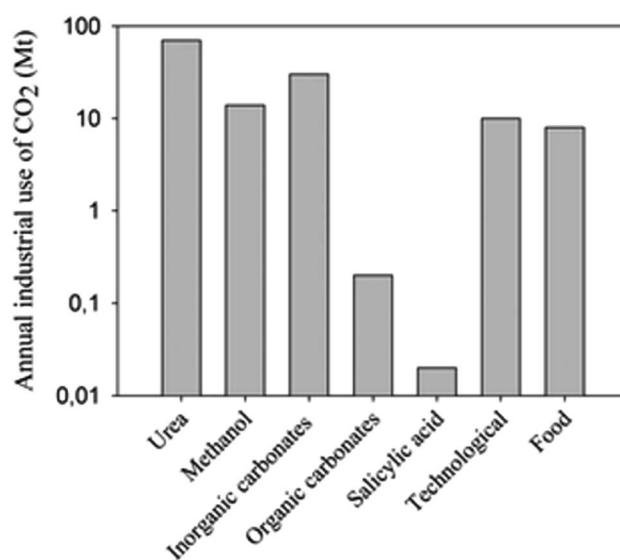

Fig. 1 CO$_2$ use in industry. Vertical axis is on logarithmic scale. Reproduced with permission from the Royal Society of Chemistry (from ref. 8).

Department of Chemical & Biomedical Engineering, University of South Florida, Tampa, FL 33620, USA. E-mail: jnkuhn@usf.edu; Tel: +1 813 974 6498

Table 1 Potential for reduction of total emissions and atmospheric influx of CO_2 using current methods and potential end products for CO_2 conversion

	Technique	Capacity of CO_2 reduction (mega tonnes CO_2 per year)	Reduction of total emissions[a]	Reduction of atmospheric CO_2 influx[b]
Current methods	Sequestration	81.5 (ref. 5)	0.25%	0.56%
	Fine chemicals synthesis	120 (ref. 8)	0.37%	0.83%
Potential uses	Plastics	155.5[c]	0.48%	1.07%
	Methanol	89.4 (ref. 22)	0.28%[d]	0.62%
	Oil derived chemicals	1200 (ref. 17)	3.73%	8.28%
	Gasoline	5364.6[e]	16.67%	37.03%

[a] Calculated using 2013 total emissions as 32.19 gigatonnes per year.[1] [b] Calculated using 14.46 gigatonnes CO_2 per year absorbed by the atmosphere (45% (ref. 2) of total 2013 emissions). [c] Estimated from the technology of Job *et al.*[14] and plastics global demand from ref. 15. [d] In accordance with ref. 16. [e] Assuming all gasoline as C_8H_{18} with a global demand of 94.83 million barrels per day (ref. 23) and a gallon yield of 45% v/v gasoline.[24]

Recently, a variety of technologies for repurposing the vastly abundant carbon dioxide into high value chemicals have emerged. To fulfill the ultimate resolution of environmental remediation, these technologies should be renewable, and the overall process needs to be carbon neutral or negative. Considering the limited sequestration capacity and the costs of CO_2 transportation and storage (~\$16.5 per tonne CO_2 (ref. 9)), developing technologies for Carbon Capture and Utilization (CCU) may make more sense than simply sequestering CO_2. However, the stability of the molecule is another challenge to overcome. CO_2 is a very stable form of carbon, making its transformation very energy intensive.

Technologies currently under research to transform CO_2 to chemicals of wide use include synthesis of polymers,[7] oxalates,[10] formates,[11] dimethyl ether,[12] ethylene and propylene[13] and an interesting recently developed technology by Job *et al.*[14] that recycles CO_2 into plastics similar to polyurethane (up to 50% CO_2 by weight). However, even at the high global demand for plastics (311 Mt in 2014 (ref. 15)), we estimate that less than 0.5% of CO_2 emissions would be used even if all the plastic produced in the world was synthesized with this technology (Table 1). Similarly, if all the methanol[16] and chemicals (made from oil)[17] consumed globally were synthesized from CO_2, emissions would not decrease by more than 0.3% and 3.8%, respectively. The comparisons of these values vividly capture the challenge of scale. The key factors of utilization still remain an issue: (i) the need for concentrated CO_2 (ref. 18 and 19) and (ii) proven technologies for conversion that can match the scale of CO_2 production and produce chemicals of significantly high demand.[18–21]

1.2   Need for energy-dense transportation fuels

In a worldwide effort to increase environmental friendliness, the use of alternative renewable technologies (such as solar, wind, geothermal, and nuclear) has been steadily increasing and evolved from representing 2.8% of the world energy production in 1973 to 8.4% in 2013.[1] The limitation is that these renewable energy sources are mostly used to generate electricity, and in 2013, electricity only represented 18.0% of the global energy consumption.[1] Renewables went from

representing 32.0% of all the electricity generated in 2011 (ref. 25) to 32.6% in 2013.[1] Unfortunately, due to intermittent supply, until new methods for efficiently storing energy generated by alternate renewable sources are developed, energy dense hydrocarbon fuels, currently produced primarily from oil, will still be necessary. Hydrocarbons store substantial chemical energy, which is not possible through various transient processes until batteries or other replacement technologies become viable.

Oil represents about 40% of the world energy consumption, and in 2013, 63.8% of all oil products were used to make transportation fuels.[1] The amount of oil products that was used to make transportation fuels increased by 44.48 Mtoe (million tonnes of oil equivalent) from 2012 (ref. 26) to 2013.[1] The demand for fuels is at least 100 times larger than chemicals.[27] Thus, only liquid fuel demand (Table 1, gasoline as example) rivals the scale of CO_2 production.[19,28,29] In other words, CO_2 emissions will continue to outweigh CO_2 consumption unless hydrocarbon transportation fuels are produced from CO_2 (closed cycle) or they are no longer required. To date, no other type of energy storage vehicle has been able to outrank the practicality of liquid fuels, making energy dense fuels still necessary.[30,31] In addition, a world-wide infrastructure for the delivery of liquid hydrocarbon fuels already exists. This avoids a major issue of the H_2 economy.

1.3   Cost estimations for CO_2 conversion processes

The need for renewable hydrogen poses a crucial problem for using the carbon of CO_2 as the backbone of future fuels.[32–37] With a minimum levelised cost of renewable electricity (produced by solar towers) of 0.17 USD per kW per h,[38] the cost of H_2 could be estimated at ~10 USD per kg H_2 (ref. 39) (as opposed to ~1.6 USD/kg H_2 if electricity was not renewable[40]). This means that if renewable H_2 was used to make one GGE of methanol, its selling price would increase by at least 4.43 USD/GGE. More recently, Kim *et al.* compared the cost of producing methanol with CO_2 splitting and different methods for obtaining H_2, one from WGS (using water and CO obtained from CO_2 splitting)[41] and the other through H_2O thermochemical splitting to H_2.[42] They determined that thermochemical splitting of

H_2O to obtain H_2 would allow for a minimal selling point of methanol at 6.73 USD/GGE[42] *vs.* using WGS, which would produce methanol at a minimum selling point of 7.10 USD/GGE.[41] Based on these back-of-the-envelope calculations, we estimate that production of renewable H_2 would contribute about 65% (4.43 USD/GGE × 100/6.73 USD/GGE) of the total methanol cost. It becomes evident that renewable H_2 synthesis is still a technology in development.[43]

1.4 Green technologies for CO_2 conversion to fuels with large demand

The technologies with the highest readiness level that are focused on converting CO_2 to synthetic fuels or their precursors (*i.e.* CO) are (i) rWGS reaction, (ii) syngas synthesis from methane dry reforming (DR) and (iii) direct hydrogenation of CO_2.

Approximately 35 megatonnes of CH_4 per year are emitted to the atmosphere from landfills.[44] If instead, this gas was trapped, it could be reacted with CO_2 in a 1 : 1 feed to produce syngas through dry reforming. Even though methane is produced at a much lower scale than CO_2 emissions, its use could be advantageous because it is produced naturally. Nonetheless, DR is an endothermic reaction,[16] favored at high temperatures (>900 °C), at which catalysts sinter and coke.[30] Often, landfill gas contains high levels of sulfur gases that cause catalyst deactivations.[16] Low temperature DR has been reported (430–470 °C) with no coking, but using an assembly of noble and transition metal catalysts combined with metal oxides (Pt–Ni–Mg/ceria–zirconia catalysts[45]) which has not yet been studied for sulfur poisoning.

Direct CO_2 hydrogenation is more thermodynamically favored than rWGS. Therefore, it was considered promising for industrialized methanol synthesis[46] and has been demonstrated on a pilot scale in Iceland by George Olah and Surya Prakash. However, the CAMERE (carbon dioxide hydrogenation to form methanol *via* reverse-water-gas-shift reaction) process revealed 20% higher methanol yields when CO_2 is converted to CO (through rWGS), and CO to methanol, rather than directly hydrogenating CO_2.[33]

Other methods, such as photo-electro-chemical reduction, are currently not a viable way to convert massive CO_2 amounts, because their low rates would highly complicate a process scale-up, which could match CO_2 production rates.[47,48] Similarly, if using biomass, the atmospheric CO_2 concentrations can only be lowered if such biomass is converted to fuels, otherwise it is not a long-term storage of CO_2.[49,50] Conversion of CO_2 to biofuels using biomass that does not compete with food and does not require land would likely involve the use of microalgae. However, the costs of cultivating and maintaining these systems would have to substantially reduce before it becomes feasible.[49–51] An upcoming technology, thermochemical CO_2 splitting, also referred to as thermochemical cycles (TCs), has the advantage of not requiring an additional reactant (other than CO_2). In this technology, CO_2 is reduced to CO on the oxygen vacancies of a metal oxide with high oxygen mobility. TCs for CO_2 splitting have been demonstrated on several oxides,[52–57] but they usually require at least 1000 °C for the formation of oxygen vacancies or several hours to be reduced at lower temperatures. On these oxygen vacant materials, the conversion of carbon dioxide to carbon monoxide has been achieved at ~900 °C.[52,54–56] The high operational temperatures would require specialized gear and an additional equipment (such as solar concentrators) that can generate the required heat input.

The rWGS is an endothermic reaction, favored at high temperatures.[36] The most commonly studied catalysts are copper-based[58–61] or supported ceria,[62–64] potentially less expensive than those used in DR. Its biggest advantage is the formation of CO, which can be used as a building block for a variety of important chemicals such as hydrocarbons in Fischer–Tropsch synthesis, fine chemical synthesis or the purification of nickel. The rWGS is suspected to be a key step in selective methanation of CO_2 (ref. 65) and to occur in FT reactors with high CO_2 feeds.[29,66] It becomes evident that rWGS is a key reaction that should be considered and fully understood.

1.5 Rationale for rWGS catalysis over competing technologies

The rWGS reaction was first observed by Carl Bosch and Wilhelm Wild in 1914, when they attempted (and halfway succeeded) to produce H_2 from steam and carbon monoxide on an iron oxide catalyst.[67] Currently, it is important in the synthesis of methanol[19] and in fixing syngas' H_2/CO ratio for various applications.

Mallapragada *et al.*[68] compared different routes to transform CO_2 into liquid fuels (biomass gasification, rWGS, algae-derived oils and direct photosynthesis) using solar assisted processes and H_2 provided by electrolysis. Among the investigated methods, conversion of CO_2 to CO by reverse water gas shift reaction followed by CO conversion to fuels with FTS had the highest current and estimated potential efficiency when CO_2 is captured from a flue gas or from the atmosphere.[68] Furthermore, converting CO_2 to CO gives an added versatility in the products that can be obtained from CO transformation.[17] The rWGS is also of great interest to be used in space exploration due high (~95%) atmospheric CO_2 concentration on Mars and availability of H_2 as a byproduct of oxygen generation.[69,70] Therefore, rWGS is a promising reaction, whose products have a wide variety of potential end uses.

The rWGS reaction is advantageous because of its technical feasibility compared to alternative technologies. However, as will be described in Section 1.6, many of the alternative technologies hold much promise if future research advances overcome significant existing challenges. In addition, with the CO_2 problem being one of such massive scale and with local resources (*e.g.*, solar insolation, available land and water) varying significantly, a multi-pronged approach is most probable, with the rWGS reaction using renewable hydrogen being one route.

1.6 Goals and limitations of this review

For the arguments already described in this review, conversion of carbon dioxide is an increasingly interesting topic for which

many critical advances are needed to make substantial contributions. The readers are directed elsewhere for superb reviews on chemical conversion to a variety of organic products,[13,36,71–75] solar-thermal-chemical cycling,[76–78] dry reforming[79–81] and other reactions with methane[82] and photo-electro-catalytic conversion.[83–87] Excellent overviews[88,89] and reviews on CO$_2$ separation[90–92] (including from air[93]) and the forward water gas shift[94] are also already available and may be of interest. Comparatively, there is very little studies summarized for the rWGS reaction even though it is a promising reaction as part of a CO$_2$ conversion system and likely the closest to implementation. Thus, the primary goal of this review is to summarize literature findings for the rWGS reaction, with an emphasis on a discussion of comparing catalyst types, rates, mechanisms, and intensification strategies. Although the forward reaction has been examined in much more depth, this review primarily focuses on literature using CO$_2$ and H$_2$ as the feed, so studies on H$_2$ purification *via* the forward WGS reaction are not included.

In addition, as a secondary goal, the scope of CO$_2$ conversion and the authors' vision for this challenge of scale has been justified in the introduction. The authors envision a society where transportation fuels and chemicals are produced from various CO$_2$ purification and conversion strategies, whereas solar, wind, and geothermal sources are employed for renewable electricity. Since CO$_2$ capture continues to be realized at various degrees, conversion strategies can operate under the assumption that CO$_2$ will be available from flue gas or atmospheric separations (taking a concentration cost but minimizing contaminant issues), which makes the conversion processes a gate-to-grave type comparison. The advantages of the rWGS reaction approach for the conversion are as follows:

• A variety of renewable electricity forms exists with various advantages occurring locally. The rWGS reaction can be implemented with any of them to contribute to a closed carbon loop.

• Hydrogen from electrolysis requires much lower capital costs than using solar-thermal-heating to magnify the low intensity solar flux to practical levels.

• The rWGS reaction produces CO, which is a very flexible chemical intermediate. Alternatively, the hydrocarbon product from photocatalysis is primarily methane, which still requires processing for use.

• Any process that generates CO still requires ~2 moles H$_2$: 1 mol CO to achieve a value-added fuel or chemical. The additional 1 mol H$_2$ for converting CO$_2$ to CO just increases the amount required from H$_2$ generation processes by 50%, not substantiating their existence in the overall process.

• Although not common, the rWGS reaction may be useful in applications where H$_2$ is readily available such as space exploration wherein electrolysis is primarily used for synthetic air production.

For these reasons and the readiness of the rWGS processes, its application in future CO$_2$ conversion strategies seems likely. To reiterate, other strategies such as a closed loop of biomass conversion are also attractive but it is unlikely that one approach would be advantageous globally. With the justification provided above, energy dense liquid hydrocarbon fuels will continue to be a transportation fuel of choice. However, transportation fuels far exceed other chemicals for contributing to the scale of the CO$_2$ problem; therefore, rWGS with methanol synthesis or FTS and biomass conversion to fuels are needed to overcome the challenge of achieving a closed carbon loop. In addition, with either synthetic (chemical) or natural (biological) CO$_2$ separation from air and conversion to plastics as a secondary, albeit smaller scale, route of conversion, it may be possible to decrease atmospheric CO$_2$ concentrations provided that electricity is available primarily from renewable sources.

2. Thermodynamic considerations

The rWGS reaction (eqn (1)) is equilibrium limited and favored at high temperatures due to the endothermic nature of the reaction.
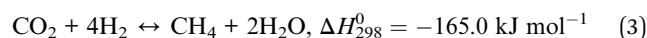
$$CO_2 + H_2 \leftrightarrow CO + H_2O, \Delta H^0_{298} = 42.1 \text{ kJ mol}^{-1} \quad (1)$$

Additional side reactions include:
Methanation

$$CO + 3H_2 \leftrightarrow CH_4 + H_2O, \Delta H^0_{298} = -206.5 \text{ kJ mol}^{-1} \quad (2)$$

and the Sabatier reaction

$$CO_2 + 4H_2 \leftrightarrow CH_4 + 2H_2O, \Delta H^0_{298} = -165.0 \text{ kJ mol}^{-1} \quad (3)$$

Thermodynamic evaluations at atmospheric pressure show that CO$_2$ conversion in the rWGS reaction is enhanced when excess H$_2$ is flowing[35] and equilibrium conversion increases with temperature[35,95] (Fig. 2). Product separation can shift the equilibrium towards the products.[27] Whitlow and Parrish from Florida Institute of Technology and NASA, respectively,[69] built a rWGS demonstration reactor without a catalyst in the system. They incorporated a membrane reactor to separate the products and achieved close to 100% CO$_2$ conversion (~5 times the equilibrium conversion). When the H$_2$/CO$_2$ flow is 0.5, CO$_2$ conversion is 1/4 lower than the equilibrium conversion with
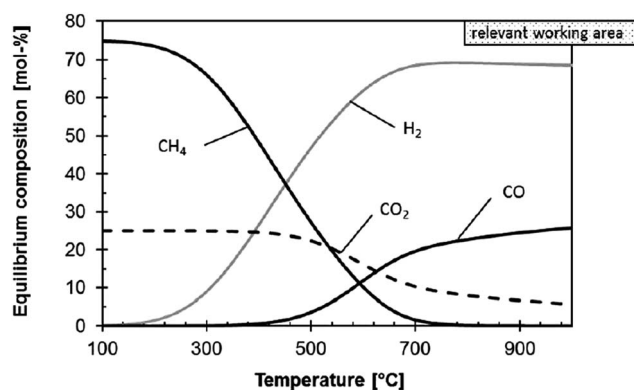

Fig. 2 Influence of temperature on the thermodynamic equilibrium of the rWGS reaction at 1 bar and H$_2$/CO$_2$ molar ratio of 3/1. Reproduced with permission from John Wiley and Sons (from ref. 17).

a 1/1 flow at the same temperature, but when the flow ratio is 2, the conversion is enhanced by 50%. Optimum operating conditions were 310 kPa and 400 °C. Medium pressures were used in the study and it was found that small variations in the pressure (131 to 310 kPa) have no effect on the conversion.[69]

In a PNNL report, VanderWiel et al.[70] studied the rWGS and Sabatier reactions for CO_2 conversion. rWGS needs to be operated at very low residence times (5 to 64 ms) to achieve the highest CO selectivity (higher than equilibrium) but a methane side product was observed in the rWGS experiments. At residence times of 32 ms, CO selectivity reaches equilibrium at ~550 °C. No CO_2 conversion was observed below 300 °C. Further ways to shift the reaction equilibrium or increase reaction rates involve the use of electricity. Applying an overpotential to the Pd-YSZ electrode increased the rate of the reaction,[96] whereas applying 3.0 mA to the 1 wt%Pt : 10 mol% La–ZrO_2 catalyst was equivalent to increasing the temperature by 100 K.[35] In both studies, CO was the only carbonaceous product.

3. Catalyst types

3.1 Supported metal catalysts

The rWGS studies of supported metal catalysts consist primarily of Cu, Pt, and Rh immobilized on a variety supports. Studies on these metals are first highlighted, and then screening studies of a wide variety of metals are discussed. Finally, support effects are reviewed.

3.1.1 Copper. The use of Cu for rWGS realizes two major advantages, (i) it has been shown to perform rWGS at low temperatures (~165 °C)[97] and (ii) little or no methane is formed as a side product.[98–100] Without hydrogen, CO_2 dissociation is highly unfavorable on clean Cu surfaces,[101–104] which directly translates into the need for high H_2/CO_2 feed ratios to achieve high CO_2 conversions. More insights into the hydrogen-aided activation will be discussed in the mechanisms section. Therefore, the enhancement of Cu activity has been extensively studied by incorporation of supports and/or promoters into the catalytic system.

Chen et al. have several contributions on the rWGS on Cu nanoparticles supported on different metal oxides. In their first study, they determined that supporting Cu NPs on Al_2O_3 increased the adsorption of formates, which they proposed as the reaction intermediates.[100] In their other contributions examining CO_2 hydrogenation on Cu nanoparticles[105] and Cu nanoparticles supported on SiO_2,[106] they also concluded that (i) the rWGS mechanism goes through a formate intermediate,[105,106] (ii) the CO_2 and CO adsorption sites for the forward and reverse mechanisms are independent,[105] and (iii) high Cu dispersion on SiO_2 enhances CO_2 conversion.[61] Ginés et al.[59] also observed that high Cu dispersion was a characteristic of the catalyst with highest activity in a Cu/ZnO/Al_2O_3 system.

Chen et al. also studied promoting the reaction with potassium[99] and iron[60,95] in the Cu/SiO_2 system. In general, promoter addition enhanced catalytic activity, but both the metals had slightly different effects. Fe prevented Cu NPs sintering, significantly enhancing the stability and activity of the

catalyst,[60,95] whereas K increased the surface active sites that can adsorb and decompose formates, enhancing the catalytic activity of the system.[99]

3.1.2 Platinum. At low temperatures (100 to 300 °C), CO_2 is converted to CO on the interface between Pt and CeO_2 after H_2 pre-treatment, but CO formation was not observed on CeO_2 or Pt alone.[107] Supported platinum (on La–ZrO_2) showed increased CO_2 conversion when compared to supported iron and copper, but lower selectivity towards CO, as demonstrated in electrically-promoted (E-rWGS) experiments.[35]

Meunier's group dominated most of the rWGS studies on Pt supported samples. The group observed different surface reactive compounds in a 2% Pt/CeO_2 catalyst depending on the reaction conditions.[108] When the reaction intermediates were allowed to accumulate under vacuum, formates were observed as the most reactive, but under steady-state conditions, the most reactive surface compounds were carbonates and carbonyls. These results shed some light on the dispute of carbonates or formates as the main reaction intermediates. High temperature DRIFT and steady-state isotopic transient kinetic analysis (SSITKA) on 2% Pt/CeO_2 confirmed that the main reaction intermediates were carbonates and not formates, although CO formation from formates could also occur in minority.[109] Observed carbonates could be mono- or bi-dentate.[107] On a solid–liquid interface, rWGS was found to occur on a Pt/Al_2O_3 system by a redox mechanism, where the O adatom (formed from CO_2 dissociation) can refill an Al_2O_3 surface vacancy or recombine with adsorbed H.[110]

The effect of adsorbed reactants and products has also been investigated in Pt systems. Jacobs and Davis[111] studied the effect of H_2O and H_2 adsorption on 1% Pt/CeO_2 during rWGS and observed different spectator species formed under different conditions, suggesting that the forward and backwards WGS mechanisms could be different. Even though Pt/SiO_2 systems have achieved higher conversion than Cu/SiO_2 at 500 °C,[61] poisoning of Pt by CO has been observed in 2% Pt/CeO_2 (ref. 112) and on Pt and Ru/Pt alloy electrodes on PEMFCs.[113] Bimetallic Co–Pt particles were tested for rWGS but it was found that Pt migrates to the surface, almost inhibiting any Co effect. The selectivity towards CO is highly increased, but there was no mention of CO_2 conversion.[114]

3.1.3 Rhodium. Rh is widely used in homogeneous CO_2 hydrogenation, mostly in amine solutions.[115] However, for Rh deposited on different supports (MgO, Nb_2O_5, ZrO_2 and TiO_2), the combined selectivity towards methane and methanol summed to more than 80% at temperatures between 100 and 300 °C and H_2/CO_2 feed ratios of 3/1.[116] Matsubu et al.[117] determined that the selectivity of CO vs. CH_4 on Rh/TiO_2 increased at low Rh loadings at 200 °C and low H_2/CO_2 feed ratios. When Rh is deposited in small loadings, it is dispersed on the surface, forming isolated Rh sites where CO_2 conversion to CO is preferred. At large loadings, Rh forms NPs, which hydrogenate CO_2 to CH_4. Similarly, high availability of H adatoms can also favor CH_4 formation.

For Rh/SiO_2, increasing the surface hydroxyl groups surrounding Rh particles on the catalyst surface increases CO_2 conversion and selectivity towards CO because it leads to
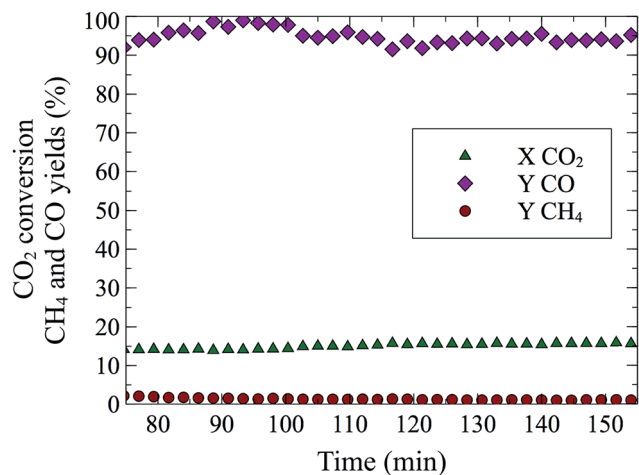
Fig. 3 Reverse water gas shift reaction over 78.3 mg of $La_{0.75}Sr_{0.25}$-FeO_3 at 550 °C. Total flow 50 sccm (10% H_2 10% CO_2 v/v, He balance). Previously, catalyst was reduced for 20 min in 10% H_2/He at 550 °C.

formation of Rh carbonyl clusters, whereas fewer hydroxyl groups form hydride species on the Rh surface, which can further hydrogenate CO to methane.[118] Li was added to an Rh ion-exchanged zeolite (Li/RhY)[119] and the selectivity towards CO (*vs.* CH_4) was found to increase with the amount of Li promoter, going from 0.3% at no Li, to 86.6% at 10 : 1 Li : Rh atomic ratio, but CO_2 conversion was decreased to half with Li addition.

3.1.4 Other transition metals and bimetallic particles or systems. Electrically promoted rWGS was performed on M/La–ZrO_2 (M = Pt, Pd, Ni, Fe, Cu) at 150 °C. CO_2 conversion was the same for Ni, Fe and Cu supported on La–ZrO_2, but 100% CO selectivity was achieved on Fe and Cu, whereas only slightly lower conversion (96.5%) was achieved on Ni.[35] DFT studies demonstrated that chemisorption energies of CO_2 are increased from early to late transition metal (Fe to Cu) (100) surfaces, but due to very strong and weak interactions with Fe (ref. 102 and 104) and Cu,[101–104] respectively, Co and Ni were deemed more favorable.[102] Experimentally, increasing Ni content in a Cu–Ni system supported on γ-Al_2O_3, had no effect on CO_2 conversion but decreased CO selectivity.[120]

Lu *et al.*[121] observed that at low NiO loadings (<3%) on CeO_2, the particles were monodispersed on the ceria matrix and lead to 100% selectivity towards CO from 400 to 750 °C, whereas higher loadings lead to aggregation and lower CO selectivity below 650 °C. Sun *et al.*[122] observed similar results on Ni/Ce–ZrO_2, increasing Ni loading decreased CO selectivity and CO_2 conversion, with the exception of 1% and 3% Ni, which exhibited similar behaviors. In conclusion, Zr appears to lower CO selectivity and CO_2 conversion.[121,122]

Wang *et al.*[64,123,124] demonstrated that different methods for supporting Ni on CeO_2 affect CO_2 conversion and CO selectivity, where the oxygen vacancies and highly dispersed surface Ni species were found to have the leading role in the reaction activity. The highest rWGS activity was observed on the catalyst synthesized by impregnation because Ni is deposited as NiO, which favors CO formation (as opposed to methane).[64] The 1% Ni/CeO_2-impregnation catalyst achieved up to 45% conversion

and 100% selectivity towards CO in a 1 : 1H_2/CO_2 flow at 750 °C.[64] Comparing this result to other studies, it appears that increasing Ni loading increases the activity of the catalyst. 2% Ni/CeO_2 showed stability for over 9 h and constant CO yield (35% in a 1 : 1H_2/CO_2 flow) at 600 °C, and 45% CO selectivity at 750 °C,[123] whereas 3% Ni/(Ce–Zr)O_2 achieved 50% CO_2 conversion and 100% CO selectivity at 750 °C (in a 1 : 1H_2/CO_2 flow) for 80 h.[122] Supporting nickel on SBA-15 did not have a significant impact on the catalyst activity,[125] but incorporation of Cu in a bimetallic Cu–Ni/SBA-15 system improved CO_2 conversion and CO selectivity,[126] as expected.

Ko *et al.*[127] also performed CO_2 dissociation DFT studies on different bimetallic alloy surfaces and determined that Fe alone and Fe-containing bimetallic particles would be the most favored to dissociate CO_2 to CO and O. Unsupported Fe-oxide NPs (10 to 20 nm) were tested for 19 h showing high stability and medium CO_2 conversion (~30%). The stability of the sample could have originated from migration of C and O into the catalyst bulk forming iron oxide and iron carbide, which likely prevented the NPs on the surface from agglomerating.[128] Kharaji *et al.*[129] determined that the supported bimetallic Mo–Fe/γ-Al_2O_3 system increased the CO formation rates, CO_2 conversion and CO selectivity when compared to the monometallic versions of the catalyst (Fe/γ-Al_2O_3 or Mo/γ-Al_2O_3).[129] The leading role of the conversion was attributed to Fe, whereas Mo enhanced the stability of iron by increasing the electron deficient state of Fe species, enhancing catalytic activity.[129] Addition of Ni to the Mo/Al_2O_3 system also showed increased activity.[130] Incorporation of Fe has also increased CO selectivity in a Rh/TiO_2 system, but greatly decreasing CO_2 conversion.[131] Porosoff *et al.*[132] showed that adding Co into Mo_2C enhances CO_2 conversion and CO selectivity at 300 °C when compared to Pt–Co and Pd–Ni bimetallic NPs supported on CeO_2. However, Ni/Mo_2C and Cu/Mo_2C have shown higher CO_2 conversion and CO selectivity than Co/Mo_2C catalysts.[133]

In_2O_3 has been found to inhibit CO production,[134] but bimetallic In–Pd NPs supported onto SiO_2 have achieved 100% CO selectivity on the rWGS,[135] although with lower activities than Pd/SiO_2. DFT suggested that the bimetallic Pd–In NPs had a weaker CO adsorption than Pd NPs, which suppresses the possibility of further hydrogenating CO to CH_4 on the bimetallic system.[135]

3.1.5 Support effects. CO formation rates on Rh supported on TiO_2 increased two orders of magnitude when compared to MgO, Nb_2O_5 and ZrO_2 as supports.[116] rWGS studies on a Pt/TiO_2 system demonstrated that TiO_2 was an active component in the reaction; H_2 reduction led to the formation of Pt–Ov–Ti^{3+} sites (Ov = oxygen vacancies).[136] The reaction activity was inversely proportional to the reducibility and crystallite size of TiO_2.[136] Sakurai *et al.*[137] compared activities in Au NPs supported on TiO_2, Al_2O_3, Fe_2O_3 and ZnO at two system pressures (P = 0.1 and 5 MPa). TiO_2 exhibited the highest activity at all reaction conditions (T = −123.15 to 126.85 °C). On this sample, CO selectivity was increased at the lowest pressure tested. Al_2O_3 and Fe_2O_3 also exhibited high activity at 0.1 MPa but it significantly decreased at 5 MPa, whereas ZnO had a low activity at both system pressures.[137]

Table 2 Rates of CO production and CO_2 conversion on different materials

Reference	Year	Material	T (°C)	P (bar)	Feed H_2/CO_2 (v/v)	CO_2 conversion (%)	CO selectivity (%)	CO formation (μmol CO per g_cat per s)
Inoue et al.[116]	1989	Rh/TiO_2	300	10.13	1/1			0.82
		$Rh-Na/TiO_2$	260					0.43
		Rh/Nb_2O_5	220					0.0
		$Rh-Na/Nb_2O_5$	200					0.05
		Rh/MgO	200					0.008
		Rh/Nb_2O_5	200		3/1			0.078
		Rh/ZrO_2	200					0.033
		Rh/TiO_2	300					0.93
Pettigrew et al.[139]	1994	Pd/Al_2O_3	260	1	1/1		78^a	0.035 (μmol CO_2 per g_cat per s)
		$Pd/La_2O_3/Al_2O_3$					70	0.027
		$Pd/PrO_2/Al_2O_3$					76	0.033
		Pd/CeO_2 (5)/Al_2O_3					87	0.045
		Pd/CeO_2 (10)/Al_2O_3					81	0.073
Ginés et al.[59]	1997	Commercial $CuO/ZnO/Al_2O_3$	250	1	$PH_2/PCO_2 = 6$	0.17		4.31
Bando et al.[119]	1998	Li/RhY (Li : Rh = 0)	250	30	3/1	24.1	0.3	
		Li/RhY (Li : Rh = 3)				12.0	3.7	
		Li/RhY (Li : Rh = 7)				11.1	27.6	
		Li/RhY (Li : Rh = 10)				13.1	86.6	
Chen et al.[100]	2000	10 wt% Cu/Al_2O_3	500	1	1/9	60		9.0
Chen et al.[95]	2001	10% Cu–0.3% Fe/SiO_2 w/w	600	1	1/1	12		
Kusama et al.[118]	2001	1 wt% Rh/SiO_2	200	50	3/1	52	88.1	
Chen et al.[99]	2003	9% Cu/SiO_2 w/w	600	1	1/1	5.3		
		9% Cu–1.9% K/SiO_2 w/w				12.8		
Chen et al.[60]	2004	0.3% Fe/SiO_2	600	1	1/1	1		
		10% Cu/SiO_2				2		
		$Cu-Fe/SiO_2$ (Cu/Fe = 10 : 0.3)				15		
		$Cu-Fe/SiO_2$ (Cu/Fe = 10 : 0.8)				16		
Goguet et al.[109]	2004	2% Pt/CeO_2 by Johnson Matthey	225		4/1	13.7		2.2×10^{-4} mol CO per g
Dorner et al.[140]	2010	Mn 12 wt%/Fe 17 wt%/Al_2O_3	290	13.8	3/1	37.7	10.7 (% CO yield)	
		Ce 2 wt%/Mn 12 wt%/Fe 17 wt%/Al_2O_3				38.6	11.5 (% CO yield)	
		Ce 10 wt%/Mn 12 wt%/Fe 17 wt%/Al_2O_3				35.8	17.5 (% CO yield)	
Gogate et al.[131]	2010	2% Rh/TiO_2	270	20.26	1/1	7.89	14.5 (% CO yield)	
		2% Rh–2.5% Fe/TiO_2				9.16	28.4 (% CO yield)	
		2.5% Fe/TiO_2				2.65	73.0 (% CO yield)	
Kim et al.[138]	2012	1% Pt/Al_2O_3	875		30/21	42		0.0104 s^{-1} (TOF at 300 °C)
		1% Pt/TiO_2				48		0.0998 s^{-1} (TOF at 300 °C)
Kim et al.[136]	2012	Pt/TiO_2 (G)^b	300			15		6480
Kharaji et al.[129]	2013	Fe/Al_2O_3	600	10	1/1		35 (% CO yield)	96.17
		Mo/Al_2O_3					33 (% CO yield)	80.14
		$Fe-Mo/Al_2O_3$					37 (% CO yield)	128.2
Lu et al.[125]	2013	NiO/SBA-15	400	1	1/1	5	100	
			900			55	100	

Table 2 (*Contd.*)

Reference	Year	Material	T (°C)	P (bar)	Feed H_2/CO_2 (v/v)	CO_2 conversion (%)	CO selectivity (%)	CO formation (µmol CO per g_cat per s)
Wang et al.[64]	2013	Ni–CeO_2	750	1	1/1	40	100	10.0 min^{-1} (TOF at ~90 °C)
Lu et al.[121]	2014	(1 wt% NiO/CeO_2)/50% wt SBA-15	750^c	1	1/1	40	100	
		(3 wt% NiO/CeO_2)/50% wt SBA-15				45	100	4.5 min^{-1} (TOF at ~90 °C)
Kim et al.[149]	2014	$BaZr_{0.8}Y_{0.2}O_3$	600		1/1	26.7	93	
		$BaZr_{0.8}Y_{0.16}Zn_{0.04}O_3$				37.5	97	
		$BaCe_{0.2}Zr_{0.6}Y_{0.16}Zn_{0.04}O_3$				36.3	94	
		$BaCe_{0.3}Zr_{0.3}Y_{0.16}Zn_{0.04}O_3$				22.3	92	
		$BaCe_{0.7}Zr_{0.1}Y_{0.16}Zn_{0.04}O_3$				10.8	74	
Oshima et al.[35,d]	2014	10% mol La–ZrO_2	150		1/1	18	100	
		1% wt Pt/10% mol La–ZrO_2				40	99.5	
		1% wt Pd/10% mol La–ZrO_2				30	98.2	
		1% wt Ni/10% mol La–ZrO_2				28	96.5	
		1% wt Fe/10% mol La–ZrO_2				28	100	
		1% wt Cu/10% mol La–ZrO_2				28	100	
Porosoff et al.[132]	2014	PtCo/CeO_2	300.85	1	2/1	6.6	4.5 (CO : CH_4 ratio)	14.6 min^{-1} (TOF)
		PdNi/CeO_2				2.5	0.6	5.6 min^{-1}
		Mo_2C				8.7	14.5	25.7 min^{-1}
		7.5 wt% Co/Mo_2C				9.5	51.3	16.1 min^{-1}
Kim et al.[128]	2015	Unsupported Fe-oxide NPs	600		1/1	38	>85	
Xu et al.[133]	2015	β-Mo_2C	200	20	5/1	6	39	
		Cu/β-Mo_2C				4	44	
		Ni/β-Mo_2C				8	37	
		Co/β-Mo_2C				9	31	
Matsubu et al.[117]	2015	0.5% w/w Rh/TiO_2	200		1/10			3.0×10^{-2} CO molecule per Rh atoms per s (TOF)
		2% w/w Rh/TiO_2						0.8
		4% w/w Rh/TiO_2						0.4
		6% w/w Rh/TiO_2						0.2
Wang et al.[62]	2016	In_2O_3	500		1/1	16		
		$In_2O_3 : CeO_2$ = 3 : 1 w/w				17		
		$In_2O_3 : CeO_2$ = 1 : 1 w/w				20		
		$In_2O_3 : CeO_2$ = 1 : 3 w/w				11		
		$In_2O_3 : CeO_2$ = 1 : 9 w/w				9		
		CeO_2				2.5		
This work	2016	$La_{0.75}Sr_{0.25}FeO_3$	550	1	1/1	15.5	95	36.4

^{a} Calculated as 100-methane selectivity. ^{b} For the meaning of G (related to origin of the support) see ref. 137. ^{c} Non steady state. ^{d} Applying 3.0 mA input current.

Between Pt/TiO$_2$ and Pt/Al$_2$O$_3$, titania exhibited higher activity and CO selectivity.[138] Different lanthanide oxides were tested as Pd supports for the reaction and the activity order was found to be CeO$_2$ > PrO$_2$ > La$_2$O$_3$.[139] When ceria has been incorporated into an Fe/Mn/Al$_2$O$_3$ system, CO selectivity was enhanced, but CO$_2$ conversion was slightly decreased.[140] Ceria is almost 100% selective towards CO at $T \geq 550$ °C,[141] most likely because at higher temperatures, the oxygen mobility of the oxide increases. Oxygen vacancies of ceria have been proven to play a leading role on the Pd/CeO$_2$/Al$_2$O$_3$ system, because they can re-oxidize with CO$_2$, whereas the role of Pd is to enhance the reduction of ceria.[139] Different shapes of cerium oxide have been tested for the rWGS and it was found that the reaction in ceria is not shape sensitive.[141] Moreover, supporting Ni on ceria slightly enhances CO$_2$ conversion but significantly improves CO selectivity,[141] as discussed in the previous section.

3.2 Oxide catalysts

The CAMERE process uses a rWGS reaction and a methanol synthesis reactor to convert CO$_2$ to methanol.[33] The first catalyst proposed on the CAMERE process consisted of Cu NPs on a ZnO/ZrO$_2$/Ga$_2$O$_3$ support at 250 °C.[33] Curiously, ZnO has been shown to be inactive for rWGS at temperatures below 165 °C.[97,142] A later CAMERE catalyst consisted of ZnO/Al$_2$O$_3$, which showed enhanced stability (tested for over 100 h) at temperatures above 700 °C.[142] The motivation for high temperatures was to favor the reaction thermodynamics. Cu was removed from the catalytic system likely because of low stability due to sample loss from the Cu oxides' reduction.[59] ZnO was tested at 600 °C for 60 h and showed high deactivation. The ZnO/Al$_2$O$_3$ catalyst exhibits less CO$_2$ conversion at 600 °C but high stability for over 200 h,[143] likely due to the formation of a ZnAl$_2$O$_4$ spinel.[142,143]

Theoretical CO$_2$ adsorption and hydrogenation studies on the In$_2$O$_3$ (110) surface suggested that In$_2$O$_3$ suppressed rWGS due to weak CO$_2$ adsorption[144] and has also been found to inhibit CO production.[134] Incorporation of CeO$_2$ in In$_2$O$_3$ increased CO$_2$ conversion (at 500 °C in a 1 : 1H$_2$/CO$_2$ flow) from 2.5% (In$_2$O$_3$) to 20% (In$_2$O$_3$: CeO$_2$, 1 : 3 w/w ratio) by increasing oxygen mobility, adsorption of CO$_2$ and generation of adsorbed bicarbonate species.[62] Similarly, incorporation of ceria into Ga$_2$O$_3$ (Ga : Ce molar ratio of 99 : 1) increased CO$_2$ conversion by 1.3% when compared to Ga$_2$O$_3$ at the same conditions described above.[63] Both studies observed increased amounts of adsorbed bicarbonate species,[62,63] which were suspected to be promoted by enhancement of oxygen mobility by ceria,[62] but neither study quantified CO selectivity or yield.

Perovskites with La on the A site and Cu[145–147] or Co[148] on the B site have been studied for CO$_2$ hydrogenation to methane and methanol. CO formation was observed by Kim et al.[149] with 97% selectivity and almost 40% CO$_2$ conversion at 600 °C and 1 bar, on a BaZr$_{0.8}$Y$_{0.16}$Zn$_{0.04}$O$_3$ oxide. With a La$_{0.75}$Sr$_{0.25}$FeO$_3$ perovskite (for synthesis method see[150]), we were able to achieve a steady state conversion of 15% at 550 °C (Fig. 3). The sample was reduced for 20 min at 10% H$_2$/He and after 20 min of flushing (100% He), the rWGS reaction (10% CO$_2$/10% H$_2$/He) was performed for 90 min. The obtained rate (1.53 millimol CO per g P per min) was three orders of magnitude larger than those of Goguet et al.[112] and Chen et al.[100] but at higher temperatures. rWGS on perovskites, BaZr$_{0.8}$Y$_{0.16}$Zn$_{0.04}$O$_3$ (ref. 149) and La$_{0.75}$Sr$_{0.25}$FeO$_3$ (this study) exhibited the added advantage of nearly 100% CO selectivity without the use of supported nanoparticles. A comparison of selectivity, conversion and different reaction conditions for multiple catalytic systems can be found in Table 2.

4. Intensified rWGS

The first attempts to achieve an intensified rWGS process emerged from combining chemical looping with DR, but substituting CH$_4$ by H$_2$ due to its higher potential as a reducing agent. In a chemical looping process, the ability of the oxygen carrier to reduce and oxidize under the desired environments is a key factor that can determine the feasibility of the process. In the rWGS process combined with chemical looping, a metal oxide is used as an oxygen carrier (Fig. 4). First, H$_2$ is used to
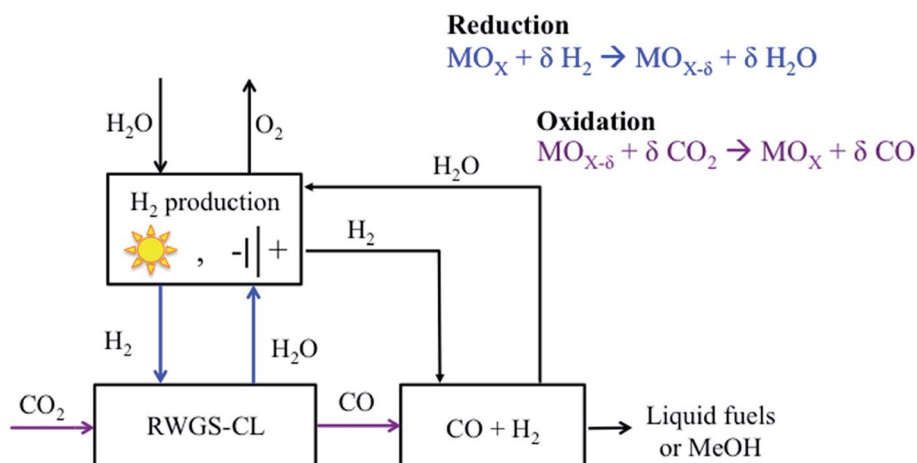

Fig. 4 Schematic of the intensified reverse water gas shift-chemical looping process (rWGS-CL). Modified with permission from the American Chemical Society (from ref. 151).

reduce the metal oxide. Subsequently, CO_2 serves as an oxidant, returning the metal oxide to an oxidized state while CO is formed. The main advantages of an intensified rWGS-chemical looping process (rWGS-CL) are eliminating the possibility of methanation because the H_2/H_2O and CO/CO_2 flows are kept separate and inherent product separation,[150–152] which drives the equilibrium towards the products. In addition, no excess hydrogen is required because the reactions involving the metal oxide are stoichiometric.

Thermodynamic modeling and experimental screening of transition metal oxides showed that Fe-based materials had one of the best CO_2 carrying capacities while having the ability to function in the widest variety of temperatures.[153,154] Najera et al.[153] observed signs of stability on a 40% w/w Fe-BHA (barium hexaaluminate) porous sample on the intensified rWGS process over 6 reaction cycles and Galvita et al.[155] used a Fe_2O_3–CeO_2 composite and found that adding ceria to iron oxide linearly enhanced the stability of the solid solution, but decreased the CO formation capabilities. The same group later studied different weight loadings of Fe_2O_3 on an Al_2O_3–MgO system and found that at low loadings of iron oxide ($\leq$30 wt%), the oxygen storage capacity of the samples decreased, but these samples are still preferred for CO_2 conversion because of the high stability of the structure that Fe, Mg and Al form during the redox cycles.[156]

The rWGS-CL process was demonstrated on $La_{(1-X)}Sr_XCoO_3$ perovskite oxides by Daza et al.,[151] but at the studied temperatures, the H_2 reduction and CO_2 conversion occurred with at least 50 °C difference, so the process was not isothermal. Reduced Fe-based spinels had been used previously for CO_2 decomposition to $C_{(s)}$ and $O_{2(g)}$ at 300 °C.[157,158] Based on this result, the rWGS-CL process was further examined using $La_{0.75}Sr_{0.25}FeO_3$ and an isothermal process at 550 °C was achieved.[150] By substituting cobalt with iron, the reducibility of the material was significantly decreased and it did not decompose under H_2 flow. However, the process was not fully stoichiometric, because even though oxygen vacancies were being created, not all the vacancies were re-filled. DFT suggested that the driving force for the CO_2 bond cleavage was the increased CO_2 adsorption strength at the highest vacancies extent tested. rWGS was tested on $La_{0.75}Sr_{0.25}Fe_{(1-Y)}Cu_YO_3$, but doping Cu into the B site of the perovskite greatly increased its reducibility and inhibited CO formation.[152]

CO formation was achieved on both cobalt- and iron-based perovskites at similar reaction conditions, but the different solid state reactions the oxides underwent suggest very different reaction pathways. The high reducibility of the Co-based perovskite[151] lead to its reduction to base La_2O_3 and metallic Co. It is likely that CO_2 then adsorbed in the basic lanthanum oxide or lanthanum-based Ruddlesden–Popper phase and dissociated in the metallic cobalt, turning the metal into cobalt oxide (CoO) while yielding CO. On the iron-based material, a surface redox mechanism between oxygen vacancies in the perovskite took place, where CO_2 was adsorbed on a lanthanum and oxygen surface termination[159] close to an oxygen vacancy, then CO_2 could dissociate into CO and an O adatom that re-fills the said oxygen vacancy.[150] Introducing Cu into the Fe-based perovskite increases the stability of the perovskite in its reduced state (after
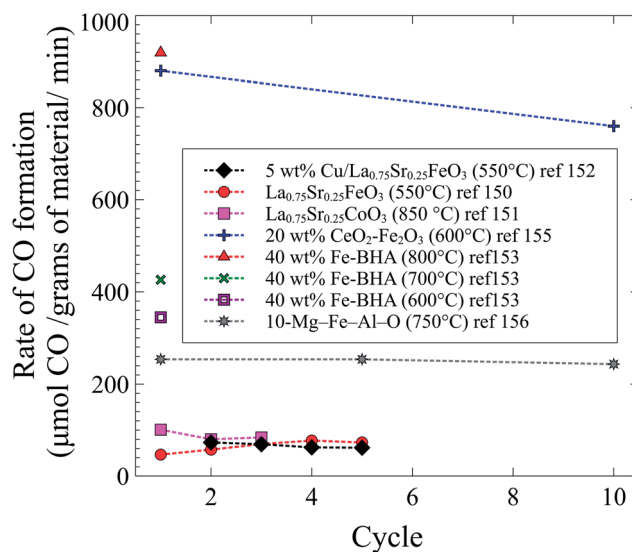

Fig. 5 CO formation as a function of cycle in the intensified rWGS-CL process from ref. 150–153, 155 and 156.

forming oxygen vacancies), therefore reducing its oxygen affinity and re-oxidation capabilities; consequently, the observed outcome was a suppression of CO production because CO_2 was not able to re-oxidized the reduced copper oxide.[152]

Throughout the different studies with an intensified version of the conventional rWGS reaction, the highest rates were achieved with Fe-containing solid solutions. A comparison of all studies covered in this section is shown in Fig. 5. Even though it has been shown before that Fe-oxides can decompose CO_2 to $C_{(s)}$ and O_2,[157,158] Fe-based oxides show the highest CO formation, and almost all materials shown in Fig. 5 contain a form of iron. Only one study has tested selectivity towards CO (vs. $C_{(s)}$) and the process is 30 times more selective towards CO.[150] As in conventional rWGS, high temperatures enhance the intensified process for CO_2 conversion. The materials with the highest CO formation rates were tested at high temperatures and with high loadings of iron. In addition to being performed at high temperatures and containing a high loading of iron, the Fe_2O_3–CeO_2 mixture exhibited the highest CO formation rates likely due to the high oxygen mobility of ceria.[155] Curiously, even though Cu is widely used as a catalyst for the forward and reverse water gas shift reactions, Fe works best for the intensified process.

5. Mechanistic considerations

5.1 Copper surfaces and supported copper nanoparticles

Studies performed on Cu surfaces[58,160] and supported Cu/ZnO systems[59] agreed that reaction orders (and therefore the rate limiting step) vary with reaction conditions. Kinetic studies over Cu (100) single crystals[58] and commercial $Cu/ZnO/Al_2O_3$ (ref. 59) demonstrated that the reaction orders with respect to P_{H_2} and P_{CO_2} change with the partial pressures of the gases.

Ernst et al.[58] and Ginés et al.[59] studied the dependence of the reaction orders for H_2 and CO_2 in the rWGS reaction. Both

studies agreed that at low P_{CO_2}/P_{H_2} (below 1/3 for ref. 59 and below 1/10 for ref. 58), the reaction rate is highly dependent on P_{CO_2} (order of ∼1.1 (ref. 59) and 0.6 (ref. 58) for CO_2) and independent of H_2 (0 order),[58,59] likely due to a deconstruction of the surface, which makes it more favorable for CO_2 dissociation.[58] At intermediate pressures ($P_{CO_2}/P_{H_2} > 1/3$ for ref. 59 and $1/10 < P_{CO_2}/P_{H_2} < 1/2$ for ref. 58), the studies disagree. Ernst et al. state that within the mentioned pressure interval, the rate depends strongly on P_{H_2} and it is independent of P_{CO_2} (0 order for P_{CO_2}), whereas Ginés et al. believe that the reaction rate is dependent on both gases (order 0.3 for P_{CO_2} and 0.8 for H_2) (Table 3). At very low P_{H_2}, the surface coverage of H_2 is lower and cannot form the favored surface;[58,59] therefore, the reaction rate is highly dependent on P_{H_2} (2nd order for P_{H_2}).[58] At higher P_{CO_2}/P_{H_2} ratios, the rate is again linearly dependent on CO_2 pressure.[58,160] High coverage of H atoms adsorbed on Cu surfaces enhance CO_2 conversion, regardless of whether hydrogen is provided as molecular hydrogen (H_2)[58] or electrochemically supplied (H^+) in solid oxide fuel cells.[161,162]

Reaction rates for the rWGS on Cu(110) and Cu(111) surfaces were comparable to Cu/ZnO except with high H_2/CO_2 partial pressure ratios. This was consistent with results showing that ZnO is not very active for rWGS[97,142] (as mentioned in Section 3.2). In the high H_2/CO_2 partial pressures case, the CO_2 decomposition mechanism seems to be aided by adsorbed H adatoms, which can adsorb in the Cu/ZnO surface but not on Cu(110) and Cu(111)[160] (Fig. 6).

Even though dissociation of CO_2 on the Cu atoms is considered as the rate determining step,[97] it is worth mentioning that the probability for CO_2 dissociation on H-adsorbed Cu surfaces is two orders of magnitude larger than on clean Cu surfaces.[160] Therefore, surface modifications by H have been suspected to favor the reaction.[160] Rates have increased by one order of magnitude when supplying electrochemical

hydrogen (H^+) in Cu electrodes in solid oxide fuel cells.[162] Furthermore, in UHV conditions, no CO_2 dissociation has been observed.[101]

In general, addition of alkali metals may alter the catalytic system reactivity.[163] Adding K as a promoter in a Cu/SiO₂ system increases the amount of active sites by increasing the positive charge on the catalyst surface,[99] which has been found favorable for the reaction because an increase in surface positive charges is less favorable for CO adsorption and its reduction to methane and other products[129] (Fig. 6).

5.2 Interactions of supported platinum nanoparticles with oxygen vacancies of supports

The rWGS mechanism on supported Pt/ceria systems has been highly debated. Jin et al.[107] determined that CO_2 is converted to CO on the interface between Pt and CeO_2 (Fig. 7), but neither on CeO_2 nor Pt alone (between 100 and 300 °C). An important observation from this study is that CO (resulting from CO_2 decomposition) is adsorbed on Pt in the same way as if CO was flowed directly.[107] This suggests that the transport and/or desorption of CO and O species (after CO_2 dissociation) is not the rate limiting step, but rather the dissociation of CO_2 itself.

Formates have been observed as the most reactive intermediate in an inert atmosphere[108] and when H_2O is included in the rWGS feed.[111] Supplying electrochemical hydrogen (H^+) in Pt[161] electrodes in solid oxide fuel cells has enhanced rWGS rates, likely supporting the claim of the formate route. Nevertheless, steady-state isotopic transient kinetic analysis (SSITKA) combined with diffuse reflectance FT-IR spectroscopy (DRIFTS) revealed that the main intermediate species are carbonates, although the reaction could also take place through minor formates and carbonyl intermediates[109] (Fig. 7). CO_2 adsorption as carbonates has also been observed on solid–liquid interfaces in the boundaries of a Pt/AlO₃ system.[110]

Table 3 Proposed rate expressions

Ref.	Catalyst	Expression	Assumption
Kaiser et al.[17]	11% Ni/Al₁₂O₁₉	$r_{m,pore} = \eta\, k_{m,CO_2}\left[C_{CO_2} - \dfrac{C_{CO}\, C_{H_2O}\, C_{H_2}{}^{-1}}{K_C}\right]$ $r_{m,ext} = \beta A_{m,ext}(C_{CO_2} - C_{CO,eq})$ $r_{m,eff} = \left[\dfrac{1}{r_{m,pore}} + \dfrac{1}{r_{m,ext}}\right]^{-1}$	Adiabatic. Only accurate if external or internal mass transport occurs, in-between regimes are approximations
Ginés et al.[59]	CuO/ZnO/Al₂O₃	$r = \dfrac{k_1\, L_0\, P^0_{CO_2}\left[P^0_{H_2}\,(1-X)^2 - \dfrac{P^0_{CO_2} X^2}{K}\right]}{P^0_{H_2}\,(1-X) + \sqrt{K_2}P^0_{H_2}\,1.5(1-X)^{1.5} + \dfrac{P^0_{CO_2} X}{K_2\, K_3}}$	CO_2 dissociation is the rate-determining step. Rate deduced from Langmuir–Hinshelwood kinetics
Chen et al.[105]	ALE-Cu/SiO₂	$r = 2^{1/2}k_4 K_1^{1/2} K_2^{1/2} K_3 P_{H_2}^{1/2} P_{CO_2}^{1/2}$	HCOO–2S → CO–S + OH–S is rate limiting[a]
Kim et al.[138,b]	Pt/TiO₂ and Pt/Al₂O₃	$r = \dfrac{k_A\, k_B\, C_t\,(P_{CO_2}\, P_{H_2} - P_{CO}\, P_{H_2O}/K_{eq})}{(k_A\, P_{CO_2} + k_{\_A}\, P_{CO} + k_B\, P_{H_2} + k_{\_B}\, P_{H_2O})}$	The adsorption of CO and H_2O was excluded and the dissociation/adsorption step was excluded at low H_2 pressure, $1 < P^0_{H_2}/P^0_{CO_2} < 4$

[a] And other mathematical assumptions. [b] Redox mechanism and associative mechanism.
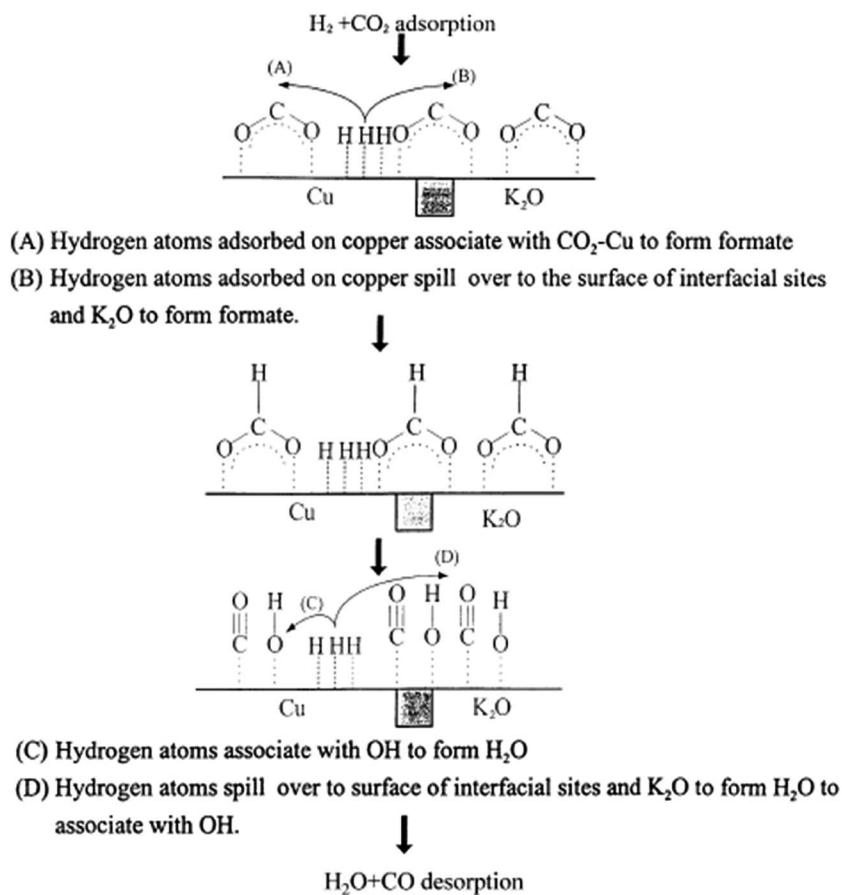
Fig. 6 Proposed rWGS mechanism on the Cu/K/SiO$_2$ interface. Reproduced with permission from Elsevier (from ref. 99).

There is, however, some agreement on the importance of the oxygen vacancies in the support. CO$_2$ is believed to adsorb on a ceria vacancy[107,109] near a platinum/ceria boundary[109] or a platinum step.[164] Goguet *et al.*[109] proposed that after CO$_2$ dissociative chemisorption (to CO and O$_a$), one O$_a$ re-fills

a vacancy and either CO is desorbed or it can migrate to the Pt surface and desorb from there[109] where the amount of CO$_2$ decomposition depends on the oxidation state of the local CeO$_2$ interface.[107] Even in solid–liquid interfaces on Pt island film deposited on a Al$_2$O$_3$ film, the mechanism for rWGS is
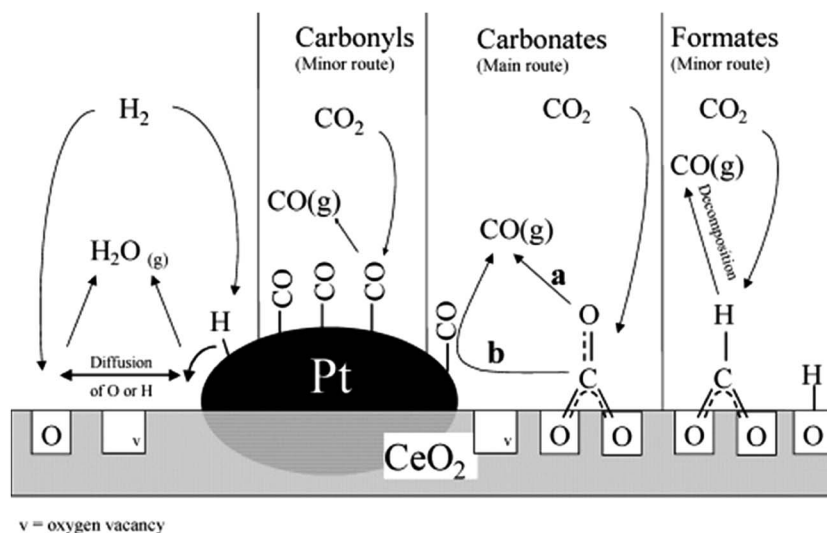

Fig. 7 Proposed rWGS mechanism on the Pt/CeO$_2$ interface. Reproduced with permission from the American Chemical Society (from ref. 109).
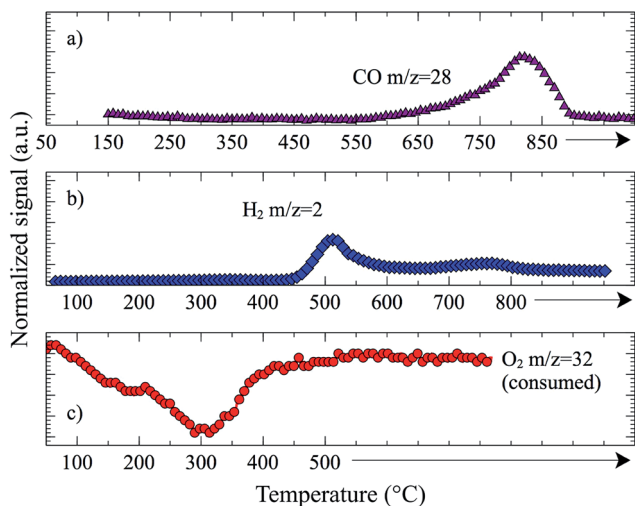
Fig. 8 Oxidation of $La_{0.75}Sr_{0.25}CoO_3$ previously reduced with 10% H_2/He at 600 °C for 30 min (total flow rate 50 sccm). (a) Oxidation with CO_2 forming CO. (b) Oxidation with H_2O forming H_2. (c) Consumption of O_2.

suspected to involve an O adatom (formed from CO_2 dissociation), which can refill an Al_2O_3 surface vacancy or recombine with adsorbed H.[110]

The redox mechanism has been proved by Kim *et al.* on Pt/TiO_2[138] and it is suspected to follow mostly a carbonate route, as described by Goguet *et al.*[109] on oxygen-mobile supports. On the contrary, on non-reductive supports (*i.e.* Al_2O_3), the carbonyl route is suspected to occur.[139]

The observation of different spectator species under different reaction conditions suggests that the forward and backwards WGS mechanisms could be different (on Pt/ceria).[111]

5.3 Role of support

Primarily, the role of support effects on the rWGS mechanism has been focused on oxygen conduction materials such as ceria and perovskite-type oxides. The Au/CeO_2 system was proven to be more active than the Au/TiO_2 due to the higher oxygen mobility of ceria[165] and its ability to be re-oxidized by CO_2.[139] This oxygen exchange can take place simultaneously (as in rWGS) or subsequently (as in rWGS-CL).[165] In_2O_3 has been shown to be promising for CO_2 hydrogenation.[144,166] On In_2O_3–CeO_2 catalysts, a volcano-type relationship between oxygen vacancies formation (increasing CeO_2) and reactive sites (increasing In_2O_3) was demonstrated.[62] When the ratio of oxides was 1 : 1, the activity of the rWGS was maximized and no side products were observed.[62] CO_2 can dissociate on the oxygen vacancies of ceria and on the Ni surface in a Ni/CeO_2 catalytic system.[141] H_2 in the reaction would form more oxygen vacancies on the ceria, but its reduction is suspected to be catalyzed by Ni,[141] similar to the mechanism on Pt/CeO_2 systems.[139]

We studied re-oxidation of pre-reduced $La_{0.75}Sr_{0.25}CoO_3$ (Fig. 8) and found that the reactivity of the oxidant was $O_2 > H_2O > CO_2$. Given the prior results from Wang *et al.*, which suggest

that the nature of the oxygen deposited on the reduced ceria surface is similar, whether it came from CO_2 or O_2 re-oxidation,[165] our results suggest that dissociation of CO_2 is the rate determining step, and not the O_a migration or H_2 dissociation, in agreement with Ernst *et al.*[58]

6. Material selection and design principles

A fair and thorough comparison of catalysts is cumbersome because experimental conditions vary widely and in a substantial number of cases, complete information is not reported (*i.e.* missing rates, conversions or yields). Supported platinum has achieved higher conversion than supported copper at 500 °C.[61] However, Cu-based catalysts are generally preferred due to their low cost, high metal abundance and because Pt is highly susceptible to CO poisoning and coke formation.[112] The poisoning effect has also been observed on Pt and Ru/Pt alloy electrodes on PEMFCs.[113] Among the supports, ceria has been shown to play a key role on the reaction due to its high oxygen mobility.[107,109,165] Furthermore, catalytic research is progressing into a material design approach, so that control of metal and support surface faceting, support vacancy amounts and locations for tuning surface properties, is probably on the horizon for rWGS catalysis.

In addition, combining Cu and ceria components seems a natural idea. Cu supported on ceria has been previously studied for CO oxidation[167,168] but recently, Rodriguez *et al.* have shown higher selectivity towards rWGS (*vs.* methanol or methane formation) on ceria supported on Cu surfaces[169] and Cu deposited on ceria and titania.[170] Therefore, it would likely be advantageous to thoroughly study Cu/ceria systems for the rWGS reaction.

7. Summary and outlook

The rWGS is a promising reaction with high potential use in the near future for the large-scale conversion of CO_2 to CO, provided that a technology for production of renewable H_2 in large scale is also available. The rWGS reaction also requires lower temperatures (~200 °C lower) than other conversion technologies that could meet the scale of CO_2 emissions. Being only slightly endothermic, the current challenge for rWGS use in fuel synthesis lies in designing materials that can achieve high CO selectivity and high production rates. Intensification strategies have recently been proposed to circumvent thermodynamic and kinetic limitations by using chemical looping to perform stoichiometric reactions rather than catalytic ones. Even though a large number of materials have been studied for the reaction, improvement is still possible. Some reports are often missing key information that allows for an equitable comparison and the effect of non-concentrated CO_2 has not been studied. Furthermore, if the rWGS reaction was to play a major role on the reduction of atmospheric CO_2 concentration, a catalyst with earth-abundant materials would be preferred.

In the interest of adopting earth-abundant metals, iron oxides could be a good substitute for ceria. Fe oxides are also known to have high oxygen mobility and stability, and when added to a Cu system, have increased the rWGS reaction activity.[60,95] In a system where Cu particles were to be supported on an iron oxide, Cu would provide high activity for CO formation, whereas Fe oxide would ideally bring high stability and high CO_2 adsorption.[104] MoC and CoMoC materials are also of interest due to their lack of precious metals and the convenience of employing industrially used metals.

Acknowledgements

References

1 International Energy Agency, 2015 Key World Energy Statistics, Supply, Consumption and Emissions, 2015, https://www.iea.org/publications/freepublications/publication/key-world-energy-statistics-2015.html.

2 U.S. Department of Energy Office of Science, U.S. DOE, Carbon Cycling and Biosequestration: Integrating Biology and Climate Through Systems Science; Report from the March 2008 Workshop, 2008, http://genomicscience.energy.gov/carboncycle/report/index.shtml.

3 J.-B. Sallee, R. J. Matear, S. R. Rintoul and A. Lenton, *Nat. Geosci.*, 2012, **5**, 579.

4 C. Hauri, T. Friedrich and A. Timmermann, *Nat. Clim. Change*, 2016, **6**, 172.

5 Global C.C.S. Institute, The Global Status of CCS: 2015, Summary Report, 2015, http://status.globalccsinstitute.com/.

6 G.C.C.S. Institute, Last access date February 17, 2016, Last updated 2015, http://www.globalccsinstitute.com/projects/large-scale-ccs-projects.

7 M. Aresta and A. Dibenedetto, *Dalton Trans.*, 2007, 2975.

8 M. Mikkelsen, M. Jorgensen and F. C. Krebs, *Energy Environ. Sci.*, 2010, **3**, 43–81.

9 J. J. Dooley, R. T. Dahowski and C. L. Davidson, *On the Long-Term Average Cost of CO_2 Transport and Storage*, U.S. Department of Energy under Contract DE-AC05-76RL01830, 2008.

10 R. Angamuthu, P. Byers, M. Lutz, A. L. Spek and E. Bouwman, *Science*, 2010, **327**, 313.

11 S. Sato, T. Arai, T. Morikawa, K. Uemura, T. M. Suzuki, H. Tanaka and T. Kajino, *J. Am. Chem. Soc.*, 2011, **133**, 15240.

12 G. A. Olah, A. Goeppert and G. K. S. Prakash, *J. Org. Chem.*, 2009, **74**, 487.

13 A. Goeppert, M. Czaun, J.-P. Jones, G. K. Surya Prakash and G. A. Olah, *Chem. Soc. Rev.*, 2014, **43**, 7995.

14 G. Job, S. D. Allen, C. Simoneau, R. Valente and J. J. Farmer, Metal complexes, *US pat.*, US20150232496A1, USA, 2015.

15 P.E.A.o.P. Manufacturers, *Plastics - the Facts 2015*, Brussels, Belgium, 2015, p. 1.

16 P. M. Mortensen and I. Dybkjær, *Appl. Catal., A*, 2015, **495**, 141.

17 P. Kaiser, R. B. Unde, C. Kern and A. Jess, *Chem.-Ing.-Tech.*, 2013, **85**, 489.

18 Department for Business, Innovation & Skills (BIS) and Department of Energy & Climate Change (DECC), E.E. Ltd, C.C. Ltd, P.S.E.P. Ltd, I. College, U.o. Sheffield, Demonstrating CO_2 capture in the UK cement, chemicals, iron and steel and oil refining sectors by 2025: A Techno-economic Study, Techno-economics of ICCS and CCU in UK, 2014, https://www.gov.uk/government/publications/co2-capture-in-the-uk-cement-chemicals-iron-steel-and-oil-refining-sectors.

19 X. Xiaoding and J. A. Moulijn, *Energy Fuels*, 1996, **10**, 305.

20 M. B. Ansari and S.-E. Park, *Energy Environ. Sci.*, 2012, **5**, 9419.

21 M. Poliakoff, W. Leitner and E. S. Streng, *Faraday Discuss.*, 2015, **183**, 9.

22 M. Institute, Last access date Last updated http://www.methanol.org/Methanol-Basics.aspx.

23 I.E. Agency, Last access date 02/22/2016, Last updated 02/09/2016, https://www.iea.org/oilmarketreport/omrpublic/.

24 U.S.E.I.A., Last access date 02/22/2016, Last updated 11/05/2015, http://www.eia.gov/Energyexplained/index.cfm?page=oil_refining.

25 International Energy Agency, 2013 Key World Energy Statistics, Transformation, 2013, http://www.iea.org/publications/freepublications/publication/KeyWorld2013_FINAL_WEB.pdf.

26 International Energy Agency, 2014 Key World Energy Statistics, Emissions, 2014, http://www.iea.org/publications/freepublications/publication/key-world-energy-statistics-2014.html.

27 G. Centi and S. Perathoner, *Catal. Today*, 2009, **148**, 191.

28 S. Chunshan, CO_2 Conversion and Utilization: An Overview, *CO_2 Conversion and Utilization*, American Chemical Society, 2002, p. 2.

29 T. Riedel, M. Claeys, H. Schulz, G. Schaub, S.-S. Nam, K.-W. Jun, M.-J. Choi, G. Kishan and K.-W. Lee, *Appl. Catal., A*, 1999, **186**, 201.

30 G. Centi, S. Perathoner and G. Iaquaniello, Realizing Resource and Energy Efficiency in Chemical Industry by Using CO_2, in *CO_2: A Valuable Source of Carbon*, ed. M. De Falco and G. Iaquaniello and G. Centi, Springer, London, 2013, p. 27.

31 S. Chu and A. Majumdar, *Nature*, 2012, **488**, 294.

32 C. Song, *Catal. Today*, 2006, **115**, 2.

33 O.-S. Joo, K.-D. Jung, I. Moon, A. Y. Rozovskii, G. I. Lin, S.-H. Han and S.-J. Uhm, *Ind. Eng. Chem. Res.*, 1999, **38**, 1808.

34 N. Meiri, Y. Dinburg, M. Amoyal, V. Koukouliev, R. V. Nehemya, M. V. Landau and M. Herskowitz, *Faraday Discuss.*, 2015, **183**, 197.

35 K. Oshima, T. Shinagawa, Y. Nogami, R. Manabe, S. Ogo and Y. Sekine, *Catal. Today*, 2014, **232**, 27.

36 W. Wang, S. Wang, X. Ma and J. Gong, *Chem. Soc. Rev.*, 2011, **40**, 3703.

37 E. V. Kondratenko, G. Mul, J. Baltrusaitis, G. O. Larrazábal and J. Pérez-Ramírez, *Energy Environ. Sci.*, 2013, **6**, 3112.

38 International Renewable Energy Agency, IRENA, Renewable Energy Cost Analysis, Concentrating Solar Power, 2012, http://www.irena.org/menu/index.aspx?mnu=Subcat&PriMenuID=36&CatID=141&SubcatID=233.

39 J. A. Turner, *Science*, 2004, **305**, 972.

40 A. Hauch, S. D. Ebbesen, S. H. Jensen and M. Mogensen, *J. Mater. Chem.*, 2008, **18**, 2331.

41 J. Kim, C. A. Henao, T. A. Johnson, D. E. Dedrick, J. E. Miller, E. B. Stechel and C. T. Maravelias, *Energy Environ. Sci.*, 2011, **4**, 3122.

42 J. Kim, T. A. Johnson, J. E. Miller, E. B. Stechel and C. T. Maravelias, *Energy Environ. Sci.*, 2012, **5**, 8417.

43 A. Taheri, E. J. Thompson, J. C. Fettinger and L. A. Berben, *ACS Catal.*, 2015, **5**, 7140.

44 U.S. E.P.A., *Global Anthropogenic Non-CO2 Greenhouse Gas Emissions: 1990–2030*, O.o.A.P.C.C. Division, U.S. Environmental Protection Agency, Washington, DC, 2012.

45 N. H. Elsayed, N. R. M. Roberts, B. Joseph and J. N. Kuhn, *Appl. Catal., B*, 2015, **179**, 213.

46 J. Skrzypek, M. Lachowska and D. Serafin, *Chem. Eng. Sci.*, 1990, **45**, 89.

47 Q. Zhai, S. Xie, W. Fan, Q. Zhang, Y. Wang, W. Deng and Y. Wang, *Angew. Chem., Int. Ed.*, 2013, **52**, 5776.

48 H. Zhou, J. Guo, P. Li, T. Fan, D. Zhang and J. Ye, *Sci. Rep.*, 2013, **3**, 1667.

49 F. G. Acién Fernández, C. V. González-López, J. M. Fernández Sevilla and E. Molina Grima, *Appl. Microbiol. Biotechnol.*, 2012, **96**, 577.

50 L. Gustavsson, P. Börjesson, B. Johansson and P. Svenningsson, *Energy*, 1995, **20**, 1097.

51 K. Gao and K. R. McKinley, *J. Appl. Phycol.*, 1994, **6**, 45.

52 W. C. Chueh, C. Falter, M. Abbott, D. Scipio, P. Furler, S. M. Haile and A. Steinfeld, *Science*, 2010, **330**, 1797.

53 P. Furler, J. R. Scheffe, M. Gorbar, L. Moes, U. Vogt and A. Steinfeld, *Energy Fuels*, 2012, **26**, 7051.

54 J. E. Miller, M. D. Allendorf, R. B. Diver, L. R. Evans, N. P. Siegel and J. N. Stuecker, *J. Mater. Sci.*, 2008, **43**, 4714–4728.

55 A. Le Gal, S. Abanades and G. Flamant, *Energy Fuels*, 2011, **25**, 4836.

56 A. H. McDaniel, E. C. Miller, D. Arifin, A. Ambrosini, E. N. Coker, R. O'Hayre, W. C. Chueh and J. Tong, *Energy Environ. Sci.*, 2013, **6**, 2024.

57 A. H. Bork, M. Kubicek, M. Struzik and J. L. M. Rupp, *J. Mater. Chem. A*, 2015, **3**, 15546.

58 K.-H. Ernst, C. T. Campbell and G. Moretti, *J. Catal.*, 1992, **134**, 66.

59 M. J. L. Ginés, A. J. Marchi and C. R. Apesteguía, *Appl. Catal., A*, 1997, **154**, 155.

60 C.-S. Chen, W.-H. Cheng and S.-S. Lin, *Appl. Catal., A*, 2004, **257**, 97.

61 C.-S. Chen, J. H. Lin, J. H. You, C. R. Chen and J. Am, *J. Am. Chem. Soc.*, 2006, **128**, 15950.

62 W. Wang, Y. Zhang, Z. Wang, J.-M. Yan, Q. Ge and C.-J. Liu, *Catal. Today*, 2016, **259**, 402.

63 B. Zhao, Y.-X. Pan and C.-J. Liu, *Catal. Today*, 2012, **194**, 60.

64 L. Wang, H. Liu, Y. Liu, Y. Chen and S. Yang, *J. Rare Earths*, 2013, **31**, 969.

65 P. Panagiotopoulou, D. I. Kondarides and X. E. Verykios, *Catal. Today*, 2012, **181**, 138–147.

66 K.-W. Jun, H.-S. Roh, K.-S. Kim, J.-S. Ryu and K.-W. Lee, *Appl. Catal., A*, 2004, **259**, 221.

67 C. Bosch and W. Wild, Producing hydrogen, *US pat.*, US1115776A, 1914.

68 D. S. Mallapragada, N. R. Singh, V. Curteanu and R. Agrawal, *Ind. Eng. Chem. Res.*, 2013, **52**, 5136.

69 J. E. Whitlow and C. F. Parrish, *AIP Conf. Proc.*, 2003, **654**, 1116–1123.

70 D. P. VanderWiel, J. L. Zilka, Y. Wang, A. Y. Tonkovich and R. S. Wegeng, Carbon Dioxide Conversions in Microreactors, IMRET 4: Proceedings of the 4th International Conference on Microreaction Technology, *Topical Conference Proceedings, AIChE Spring National Meeting*, American Institute of Chemical Engineers, Atlanta, GA, 2000, p. 187.

71 M. D. Porosoff, B. Yan and J. G. Chen, *Energy Environ. Sci.*, 2016, **9**, 62.

72 P. Lanzafame, G. Centi and S. Perathoner, *Chem. Soc. Rev.*, 2014, **43**, 7562.

73 G. Centi, E. A. Quadrelli and S. Perathoner, *Energy Environ. Sci.*, 2013, **6**, 1711.

74 W. Wang and J. Gong, *Front. Chem. Sci. Eng.*, 2011, **5**, 2.

75 T. Sakakura, J.-C. Choi and H. Yasuda, *Chem. Rev.*, 2007, **107**, 2365.

76 N. P. Siegel, J. E. Miller, I. Ermanoski, R. B. Diver and E. B. Stechel, *Ind. Eng. Chem. Res.*, 2013, **52**, 3276.

77 G. P. Smestad and A. Steinfeld, *Ind. Eng. Chem. Res.*, 2012, **51**, 11828.

78 T. Kodama and N. Gokon, *Chem. Rev.*, 2007, **107**, 4048.

79 J. R. Rostrup-Nielsen and J. Sehested, *Adv. Catal.*, 2002, **47**, 65.

80 M. C. J. Bradford and M. A. Vannice, *Catal. Rev.–Sci. Eng.*, 1999, **41**, 1.

81 D. Pakhare and J. J. Spivey, *Chem. Soc. Rev.*, 2014, **43**, 7813.

82 V. Havran, M. P. Dudukovi and C. S. Lo, *Ind. Eng. Chem. Res.*, 2011, **50**, 7089.

83 E. V. Kondratenko, G. Mul, J. Baltrusaitis, G. O. Larrazabal and J. Perez-Ramírez, *Energy Environ. Sci.*, 2013, **6**, 3112.

84 S. N. Habisreutinger, L. Schmidt-Mende and J. K. Stolarczyk, *Angew. Chem., Int. Ed.*, 2013, **52**, 7372.

85 B. Kumar, M. Llorente, J. Froehlich, T. Dang, A. Sathrum and C. P. Kubiak, *Annu. Rev. Phys. Chem.*, 2012, **63**, 541.

86 S. C. Roy, O. K. Varghese, P. Paulose and C. A. Grimes, *ACS Nano*, 2010, 1259.

87 V. P. Indrakanti, J. D. Kubicki and H. H. Schobert, *Energy Environ. Sci.*, 2009, **2**, 745.

88 A. M. Appel, J. E. Bercaw, A. B. Bocarsly, H. Dobbek, D. L. DuBois, M. Dupuis, J. G. Ferry, E. Fujita, R. Hille, P. J. A. Kenis, C. A. Kerfeld, R. H. Morris, C. H. F. Peden, A. R. Portis, S. W. Ragsdale, T. B. Rauchfuss,

J. N. H. Reek, L. C. Seefeldt, R. K. Thauer and G. L. Waldrop, *Chem. Rev.*, 2013, **113**, 6621.

89 H. Arakawa, M. Aresta, J. N. Armor, M. A. Barteau, E. J. Beckman, A. T. Bell, J. E. Bercaw, C. Creutz, E. Dinjus, D. A. Dixon, K. Domen, D. L. DuBois, J. Eckert, E. Fujita, D. H. Gibson, W. A. Goddard, D. W. Goodman, J. Keller, G. J. Kubas, H. H. Kung, J. E. Lyons, L. E. Manzer, T. J. Marks, K. Morokuma, K. M. Nicholas, R. Periana, L. Que, J. Rostrup-Nielson, W. M. H. Sachtler, L. D. Schmidt, A. Sen, G. A. Somorjai, P. C. Stair, B. R. Stults and W. Tumas, *Chem. Rev.*, 2001, **101**, 953.

90 N. von der Assen, P. Voll, M. Peters and A. Bardow, *Chem. Soc. Rev.*, 2014, **43**, 7982.

91 L.-S. Fan, L. Zeng, W. Wang and S. Luo, *Energy Environ. Sci.*, 2012, **5**, 7254.

92 N. MacDowell, N. Florin, A. Buchard, J. Hallett, A. Galindo, G. Jackson, C. S. Adjiman, C. K. Williams, N. Shah and P. Fennell, *Energy Environ. Sci.*, 2010, **3**, 1645.

93 G. Goeppert, M. Czaun, G. K. S. Prakash and G. A. Olah, *Energy Environ. Sci.*, 2012, **5**, 7833.

94 C. Ratnasamy and J. P. Wagner, *Catal. Rev.*, 2009, **51**, 325.

95 C.-S. Chen, W.-H. Cheng and S.-S. Lin, *Chem. Commun.*, 2001, 1770.

96 S. Bebelis, H. Karasali and C. G. Vayenas, *Solid State Ionics*, 2008, **179**, 1391.

97 S.-I. Fujita, M. Usui and N. Takezawa, *J. Catal.*, 1992, **134**, 220.

98 J. A. Rodriguez, J. Evans, L. Feria, A. B. Vidal, P. Liu, K. Nakamura and F. Illas, *J. Catal.*, 2013, **307**, 162.

99 C.-S. Chen, W.-H. Cheng and S.-S. Lin, *Appl. Catal., A*, 2003, **238**, 55.

100 C.-S. Chen, W.-H. Cheng and S.-S. Lin, *Catal. Lett.*, 2000, **68**, 45.

101 J. Nakamura, J. A. Rodriguez and C. T. Campbell, *J. Phys.: Condens. Matter*, 1989, **1**, Sb149.

102 C. Liu, T. R. Cundari and A. K. Wilson, *J. Phys. Chem. C*, 2012, **116**, 5681.

103 S.-G. Wang, X.-Y. Liao, D.-B. Cao, C.-F. Huo, Y.-W. Li, J. Wang and H. Jiao, *J. Phys. Chem. C*, 2007, **111**, 16934.

104 T. Bligaard, J. K. Nørskov, S. Dahl, J. Matthiesen, C. H. Christensen and J. Sehested, *J. Catal.*, 2004, **224**, 206.

105 C.-S. Chen, J. H. Wu and T. W. Lai, *J. Phys. Chem. C*, 2010, **114**, 15021.

106 C.-S. Chen and W.-H. Cheng, *Catal. Lett.*, 2002, **83**, 121.

107 T. Jin, Y. Zhou, G. J. Mains and J. M. White, *J. Phys. Chem.*, 1987, **91**, 5931–5937.

108 D. Tibiletti, A. Goguet, F. Meunier, J. P. Breen and R. Burch, *Chem. Commun.*, 2004, 1636.

109 A. Goguet, F. C. Meunier, D. Tibiletti, J. P. Breen and R. Burch, *J. Phys. Chem. B*, 2004, **108**, 20240.

110 D. Ferri, T. Bürgi and A. Baiker, *Phys. Chem. Chem. Phys.*, 2002, **4**, 2667.

111 G. Jacobs and B. H. Davis, *Appl. Catal., A*, 2005, **284**, 31.

112 A. Goguet, F. Meunier, J. P. Breen, R. Burch, M. I. Petch and A. F. Ghenciu, *J. Catal.*, 2004, **226**, 382.

113 T. Gu, W.-K. Lee and J. W. Van Zee, *Appl. Catal., B*, 2005, **56**, 43.

114 S. Alayoglu, S. K. Beaumont, F. Zheng, V. V. Pushkarev, H. Zheng, V. Iablokov, Z. Liu, J. Guo, N. Kruse and G. A. Somorjai, *Top. Catal.*, 2011, **54**, 778.

115 P. G. Jessop, F. Joó and C.-C. Tai, *Coord. Chem. Rev.*, 2004, **248**, 2425.

116 T. Inoue, T. Iizuka and K. Tanabe, *Appl. Catal.*, 1989, **46**, 1.

117 J. C. Matsubu, V. N. Yang and P. Christopher, *J. Am. Chem. Soc.*, 2015, **137**, 3076.

118 H. Kusama, K. K. Bando, K. Okabe and H. Arakawa, *Appl. Catal., A*, 2001, **205**, 285.

119 K. K. Bando, K. Soga, K. Kunimori and H. Arakawa, *Appl. Catal., A*, 1998, **175**, 67.

120 Y. Liu and D. Liu, *Int. J. Hydrogen Energy*, 1999, **24**, 351.

121 B. Lu and K. Kawamoto, *Mater. Res. Bull.*, 2014, **53**, 70.

122 F.-M. Sun, C.-F. Yan, Z.-D. Wang, C.-Q. Guo and S.-L. Huang, *Int. J. Hydrogen Energy*, 2015, **40**, 15985.

123 L. Wang, S. Zhang and Y. Liu, *J. Rare Earths*, 2008, **26**, 66.

124 L. Wang, H. Liu, Y. Liu, Y. Chen and S. Yang, *J. Rare Earths*, 2013, **31**, 559.

125 B. Lu, K. Kawamoto and J. Environ, *Chem. Eng.*, 2013, **1**, 300.

126 B. Lu, Y. Ju, T. Abe and K. Kawamoto, *Inorg. Chem. Front.*, 2015, **2**, 741.

127 J. Ko, B.-K. Kim and J. W. Han, *J. Phys. Chem. C*, 2016, **120**, 3438.

128 D. H. Kim, S. W. Han, H. S. Yoon and Y. D. Kim, *J. Ind. Eng. Chem.*, 2015, **23**, 67.

129 A. G. Kharaji, A. Shariati and M. A. Takassi, *Chin. J. Chem. Eng.*, 2013, **21**, 1007.

130 A. G. Kharaji, A. Shariati, M. Ostadi and J. Nanosci, *J. Nanotechnol.*, 2014, **14**, 6841.

131 M. R. Gogate and R. J. Davis, *Catal. Commun.*, 2010, **11**, 901.

132 M. D. Porosoff, X. Yang, A. J. Boscoboinik and J. G. Chen, *Angew. Chem., Int. Ed.*, 2014, **126**, 6823.

133 W. Xu, P. J. Ramírez, D. Stacchiola, J. L. Brito and J. A. Rodriguez, *Catal. Lett.*, 2015, **145**, 1365.

134 T. Umegaki, K. Kuratani, Y. Yamada, A. Ueda, N. Kuriyama, T. Kobayashi and Q. Xu, *J. Power Sources*, 2008, **179**, 566.

135 J. Ye, Q. Ge and C.-J. Liu, *Chem. Eng. Sci.*, 2015, **135**, 193.

136 S. S. Kim, H. H. Lee and S. C. Hong, *Appl. Catal., B*, 2012, **119–120**, 100.

137 H. Sakurai, A. Ueda, T. Kobayashi and M. Haruta, *Chem. Commun.*, 1997, 271–272.

138 S. S. Kim, H. H. Lee and S. C. Hong, *Appl. Catal., A*, 2012, **423–424**, 100.

139 D. J. Pettigrew, D. L. Trimm and N. W. Cant, *Catal. Lett.*, 1994, **28**, 313.

140 R. W. Dorner, D. R. Hardy, F. W. Williams and H. D. Willauer, *Catal. Commun.*, 2010, **11**, 816.

141 Y. Liu, Z. Li, H. Xu and Y. Han, *Catal. Commun.*, 2016, **76**, 1.

142 S.-W. Park, O.-S. Joo, K.-D. Jung, H. Kim and S.-H. Han, *Appl. Catal., A*, 2001, **211**, 81.

143 O.-S. Joo and K.-D. Jung, *Bull. Korean Chem. Soc.*, 2003, **24**, 86.

144 J. Ye, C. Liu and Q. Ge, *J. Phys. Chem. C*, 2012, **116**, 7817.

145 L. Jia, J. Gao, W. Fang and Q. Li, *J. Rare Earths*, 2010, **28**, 747.

146 H. Zhan, F. Li, P. Gao, N. Zhao, F. Xiao, W. Wei, L. Zhong and Y. Sun, *J. Power Sources*, 2014, **251**, 113.

147 L. Jia, J. Gao, W. Fang and Q. Li, *Catal. Commun.*, 2009, **10**, 2000.

148 M. A. Ulla, R. A. Migone, J. O. Petunchi and E. A. Lombardo, *J. Catal.*, 1987, **105**, 107.

149 D. H. Kim, J. L. Park, E. J. Park, Y. D. Kim and S. Uhm, *ACS Catal.*, 2014, **4**, 3117.

150 Y. A. Daza, D. Maiti, R. A. Kent, V. R. Bhethanabotla and J. N. Kuhn, *Catal. Today*, 2015, **258**, 691.

151 Y. A. Daza, R. A. Kent, M. M. Yung and J. N. Kuhn, *Ind. Eng. Chem. Res.*, 2014, **53**, 5828.

152 Y. A. Daza, D. Maiti, B. J. Hare, V. R. Bhethanabotla and J. N. Kuhn, *Surf. Sci.*, 2016, **648**, 92.

153 M. Najera, R. Solunke, T. Gardner and G. Veser, *Chem. Eng. Res. Des.*, 2011, **89**, 1533.

154 R. D. Solunke and G. Veser, *Ind. Eng. Chem. Res.*, 2010, **49**, 11037.

155 V. V. Galvita, H. Poelman, V. Bliznuk, C. Detavernier and G. B. Marin, *Ind. Eng. Chem. Res.*, 2013, **52**, 8416.

156 N. V. R. A. Dharanipragada, L. C. Buelens, H. Poelman, E. D. Grave, V. V. Galvita and G. B. Marin, *J. Mater. Chem. A*, 2015, **3**, 16251.

157 C. Nordhei, K. Mathisen, I. Bezverkhyy and D. G. Nicholson, *J. Phys. Chem.*, 2008, **112**, 6531–6537.

158 C. Nordhei, K. Mathisen, O. Safonova, W. van Beek and D. G. Nicholson, *J. Phys. Chem.*, 2009, **113**, 19568.

159 D. Maiti, Y. A. Daza, M. M. Yung, J. N. Kuhn and V. R. Bhethanabotla, *J. Mater. Chem. A*, 2016, **4**, 5137.

160 C. T. Campbell and K.-H. Ernst, Forward and Reverse Water-Gas Shift Reactions on Model Copper Catalysts, *Surface Science of Catalysis*, American Chemical Society, 1992, p. 130.

161 G. Pekridis, K. Kalimeri, N. Kaklidis, E. Vakouftsi, E. F. Iliopoulou, C. Athanasiou and G. E. Marnellos, *Catal. Today*, 2007, **127**, 337.

162 G. Karagiannakis, S. Zisekas and M. Stoukides, *Solid State Ionics*, 2003, **162–163**, 313.

163 F. Solymosi, *J. Mol. Catal.*, 1991, **65**, 337.

164 J. Xu and J. T. Yates Jr, *Surf. Sci.*, 1995, **327**, 193–201.

165 L. C. Wang, M. Tahvildar Khazaneh, D. Widmann and R. J. Behm, *J. Catal.*, 2013, **302**, 20.

166 Q. Sun, J. Ye, C.-J. Liu and Q. Ge, *Greenhouse Gases: Sci. Technol.*, 2014, **4**, 140–144.

167 D. Gamarra, G. Munuera, A. B. Hungría, M. Fernández-García, J. C. Conesa, P. A. Midgley, X. Q. Wang, J. C. Hanson, J. A. Rodríguez and A. Martínez-Arias, *J. Phys. Chem. C*, 2007, **111**, 11026.

168 N. E. Nunez, H. P. Bideberripe, M. L. Casella and G. J. Siri, *Curr. Catal.*, 2014, **3**, 187.

169 J. A. Rodriguez, P. Liu, D. J. Stacchiola, S. D. Senanayake, M. G. White and J. G. Chen, *ACS Catal.*, 2015, **5**, 6696.

170 J. Graciani, K. Mudiyanselage, F. Xu, A. E. Baber, J. Evans, S. D. Senanayake, D. J. Stacchiola, P. Liu, J. Hrbek, J. Fernández-Sanz and J. A. Rodriguez, *Science*, 2014, **345**, 546.